Supplementary Information

Dynamics of nucleosome remodelling by individual ACF complexes

Timothy R. Blosser, Janet G. Yang, Michael D. Stone, Geeta J. Narlikar,

and Xiaowei Zhuang

Supplementary Information Contents:

Supplementary Figure 12: Intensity and photobleaching step analyses of dye-labeled ACF associated with the unidirectional and bidirectional nucleosome remodelling events.

Supplementary Figures:

Supplementary Figure 1. DNA sequences used to construct nucleosomes in this work. a, DNA sequences containing the 601 positioning sequence (blue)[24] with a PstI restriction site modification (red)[23], 78 bp of linker DNA on the entry side, and various lengths of linker DNA on the exit side (*n* = -3 bp, 0 bp, 3 bp, 6 bp and 78 bp). The *n* = -3 bp case corresponds to the first 3 base pairs missing from the 601 sequence on the exit side. **b**, A DNA sequence taken from a region of the pFastBac1 bacterial plasmid[32]. This DNA sequence, referred to as "ARB" previously[32] and "A-100" in this work, has ~100-fold lower affinity for a histone octamer than the 601 sequence[32].

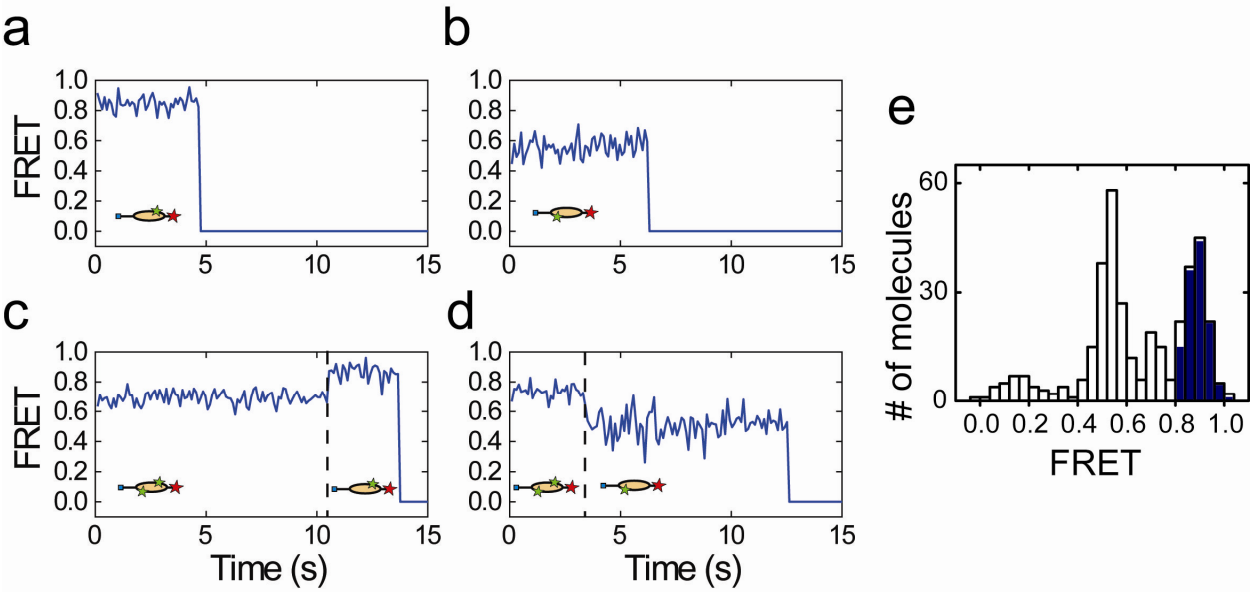

Supplementary Figure 2. Assignment of the FRET = 0.88, 0.75 and 0.58 levels to the three donor labelling configurations for the *n* = 3 bp nucleosomes. The FRET donor Cy3 (green star) can be attached to two sites on the histone octamer, one of which is on the H2A subunit proximal to the FRET acceptor Cy5 (red star) on the DNA and the other is on the H2A subunit distal to Cy5. **a**, Histone octamers labelled with a single Cy3 on the proximal H2A exhibit a high FRET level at 0.88 and single-step photobleaching of Cy3. After donor bleaching, the FRET level is assigned to zero. **b**, Octamers labelled with a single Cy3 on the distal H2A exhibit a relatively low FRET level at 0.58 and single-step photobleaching of Cy3. **c** and **d**, Octamers labelled with two Cy3 dyes (on both the proximal and distal H2A) initially exhibit an intermediate FRET level at 0.75 and two-step photobleaching of the Cy3 signal. After the first bleaching step (dotted line), fluorescence from a single Cy3 dye remained from either the proximal H2A, exhibiting a FRET = 0.88 intermediate before the second bleaching step (**c**), or the distal H2A, exhibiting a FRET = 0.58 intermediate before the second bleaching step (**d**). **e**, FRET histogram (hollow bars) derived from the starting mean FRET value of many FRET traces as shown in (a)-(d). The histogram shows three main peaks at 0.88, 0.75 and 0.58. To establish criteria for selecting nucleosomes with a single FRET donor on the proximal H2A, traces starting with a mean FRET > 0.75 and exhibiting a single donor bleaching step were selected. The histogram of the starting FRET values of these traces is shown in solid bars. As expected, such a selection process resulted in a single population of nucleosomes centred at FRET = 0.88.

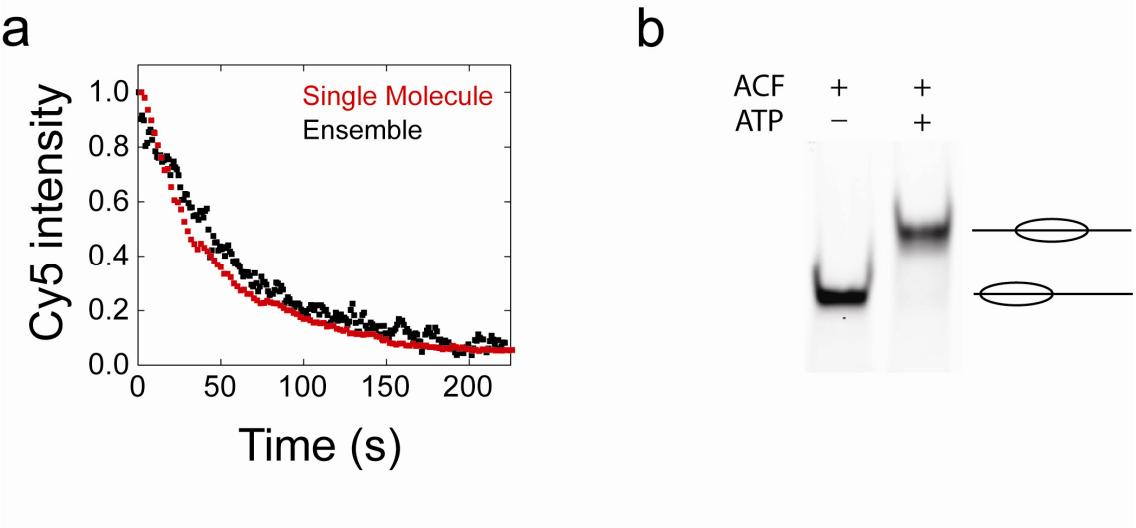

Supplementary Figure 3. Comparison of nucleosome remodelling measured by the single-molecule FRET assay and ensemble experiments. a, The overall remodelling kinetics measured by single-molecule FRET for surface-anchored nucleosomes are compared with results from an ensemble FRET measurement performed on freely diffusing nucleosomes in a solution. The single-molecule data (red) were obtained by taking the average Cy5 intensity of more than 500 single-nucleosome time traces as shown in Fig. 2a. The ensemble data (black) represent the total acceptor signal from a solution of 2 nM nucleosomes measured by a fluorimeter. In both cases, 4 nM ACF and 20 μM ATP were added to the nucleosome samples to initiate the remodelling reaction. As the nucleosomes were translocated to the center of the DNA, the FRET value decreased, resulting in a decrease in the acceptor Cy5 signal. The quantitatively similar time courses of the Cy5 signal in both cases indicate that surface anchoring of the nucleosomes did not inhibit the remodelling activity of ACF. **b**, Native gel electrophoresis shows that the FRET-labelled nucleosomes after remodelling remained intact, exhibiting an expected retardation in electrophoretic mobility as compare to the nucleosomes before remodelling, consistent with previous gel electrophoresis on unlabelled and similarly labelled mononucleosomes[23].

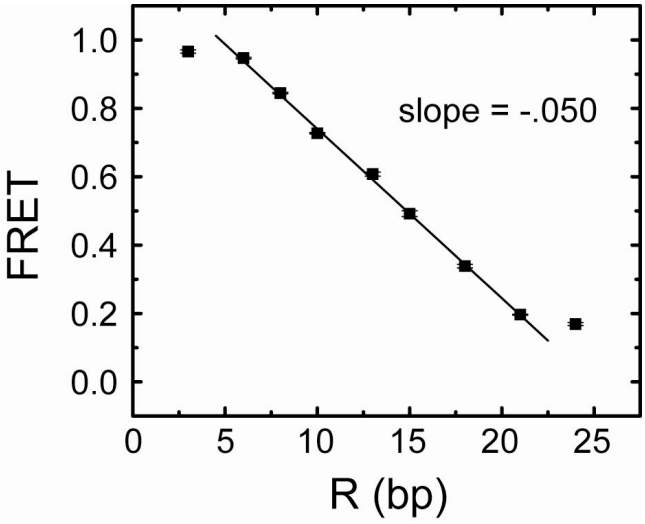

Supplementary Figure 4: Distance dependence of FRET measured on double-stranded DNA. For this experiment, we constructed a series of duplex-DNA sample (alone without attached histone octamer) with different dye labeling sites. A FRET acceptor (Cy5) was attached to the end of one DNA strand, while the FRET donor (Cy3) was attached to an internal site on the opposite DNA strand. For different duplex DNA samples, the donor-acceptor separation R was varied and measured in base-pairs. The observed FRET value as a function of the donor-acceptor separation shows a similar dependence to that observed for the nucleosome calibration samples (Fig. 1c): the FRET value shows a roughly linear dependence on the donor-acceptor separation over a large FRET range; both the linear range and its slope are similar to those of the nucleosome calibration samples. The deviation from the expected nonlinear dependence is likely due to the flexible linkers connecting the dyes to the DNA or nucleosome. Indeed, a simulation shows that the FRET efficiency exhibits a sharp nonlinear dependence on the dye separation when the FRET dyes are directly connected to the DNA, whereas in the case where the dyes are connected to the DNA via a flexible linker, the distance dependence becomes shallower and appears linear over a larger distance range (data not shown). In the simulation, the attachment sites of the dyes were determined from the crystals structure of double-stranded DNA and the positions of the dyes were simulated by a diffusive probability density with maximum distance from the attachment site defined by the linker length. Error bars are ± s.e.m.

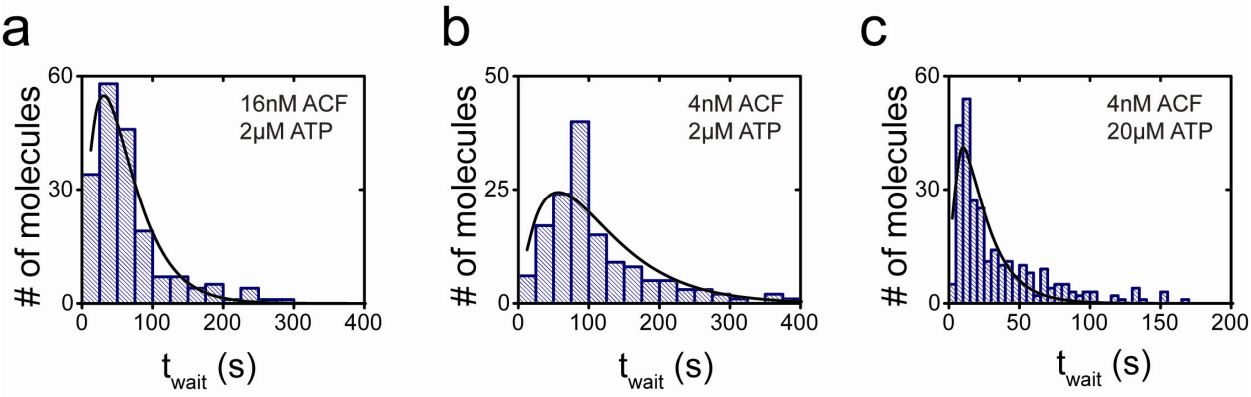

Supplementary Figure 5. Distributions of t_{wait} at various ATP and ACF concentrations. a, 16 nM ACF and 2 μM ATP. **b**, 4 nM ACF and 2 μM ATP. **c**, 4 nM ACF and 20 μM ATP. The mean values of t_{wait} at these and additional ACF and ATP concentrations are shown in Fig. 2b. The distribution of t_{wait} at the lowest ACF and ATP concentrations (**b**) exhibits a pronounced lag, indicating that the waiting phase consists of at least two steps. The lag decreased as either the ACF (**a**) or the ATP (**c**) concentration was increased, suggesting that one of the two steps is ACF dependent and the other is ATP dependent. These distributions were fit to a lagged exponential with two rate constants: # of molecules = $A[\exp(-k_1 t) - \exp(-k_2 t)]$. The two rate constants (k_1, k_2) are (0.018 s^{-1}, 0.018 s^{-1}) at 4 nM ACF and 2 μM ATP, and (0.06 s^{-1}, 0.16 s^{-1}) at 4 nM ACF and 20 μM ATP. These results are comparable to the rate constants $1/t_{bind}$ and $1/t_{lag}$ derived at the same ACF and ATP concentrations from a more direct kinetic analysis by simultaneously monitoring the binding of ACF and the FRET from the nucleosome (Fig. 2c). From the distributions shown in Fig. 2c, we derived ($1/\langle t_{bind} \rangle$, $1/\langle t_{lag} \rangle$) = (0.024 s^{-1}, 0.023 s^{-1}) at 4 nM ACF and 2 μM ATP, and (0.05 s^{-1}, 0.1 s^{-1}) at 4 nM ACF and 20 μM ATP.

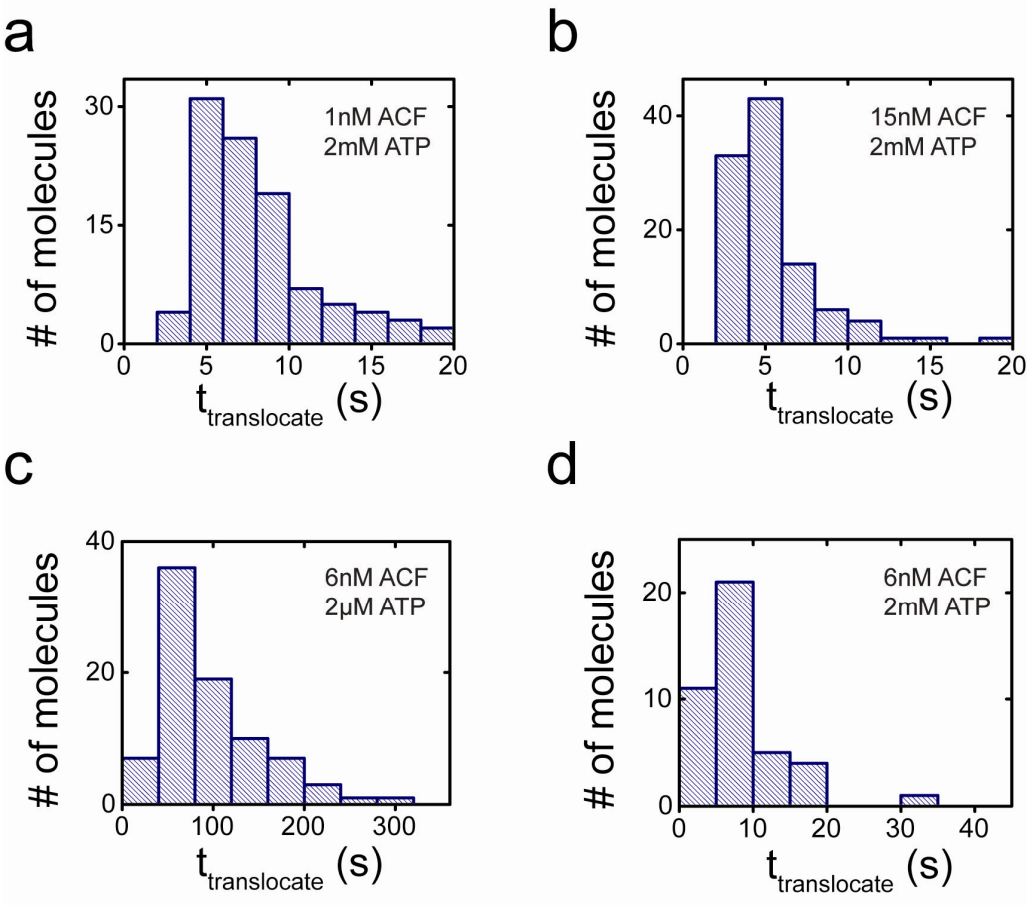

Supplementary Figure 6. Distributions of $t_{translocate}$ at various ATP and ACF concentrations. **a**, 1 nM ACF and 2 mM ATP. **b**, 15 nM ACF and 2 mM ATP. **c**, 6 nM ACF and 2 μM ATP. **d**, 6 nM ACF and 2 mM ATP. The distributions of $t_{translocate}$ appear similar at different ACF concentrations but distinct at different ATP concentrations (note the different time axes). The mean values of $t_{translocate}$ at these and additional ACF and ATP concentrations are shown in Fig. 2d.

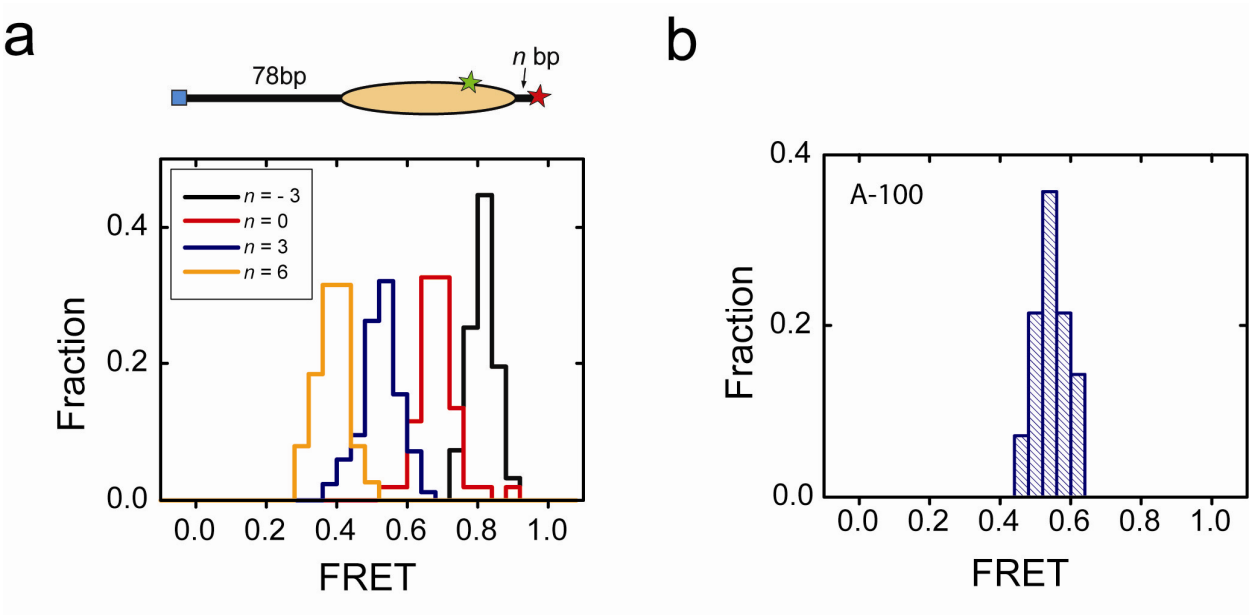

Supplementary Figure 7. The first translocation pause for nucleosomes with different exit linker DNA lengths and different DNA sequences. a, FRET histogram of the first translocation pause for nucleosomes with the 601 positioning sequence and different initial exit linker lengths (*n* = -3, 0, 3 and 6 bp, See supplementary Fig. 1a). The mean FRET value of the first translocation pause in each remodelling trace was used to construct the histograms. The pause FRET values for the *n* = -3, 0, 3 and 6 bp constructs correspond to an exit linker length of 4.3, 6.9, 9.9 and 12.6 bp, respectively, and thus translocation of 7.3, 6.9, 6.9 and 6.6 bp prior to the pause, respectively. **b**, FRET histogram of the first translocation pause for nucleosomes with the "A-100" sequence (See supplementary Fig. 1b). The A-100 sequence largely positions the octamer near the end of the DNA, but with ~100 fold lower affinity than the 601 sequence. To allow for a direct comparison with the *n* = 3 bp nucleosome positioned by the 601 sequence (initial FRET = 0.88), FRET traces of the A-100 nucleosomes that started with an initial FRET = 0.88 ± 0.05 were selected for pause analysis. The mean pause FRET value was found to be 0.54 ± 0.05, which corresponds to ~7 bp of translocation prior to the pause.

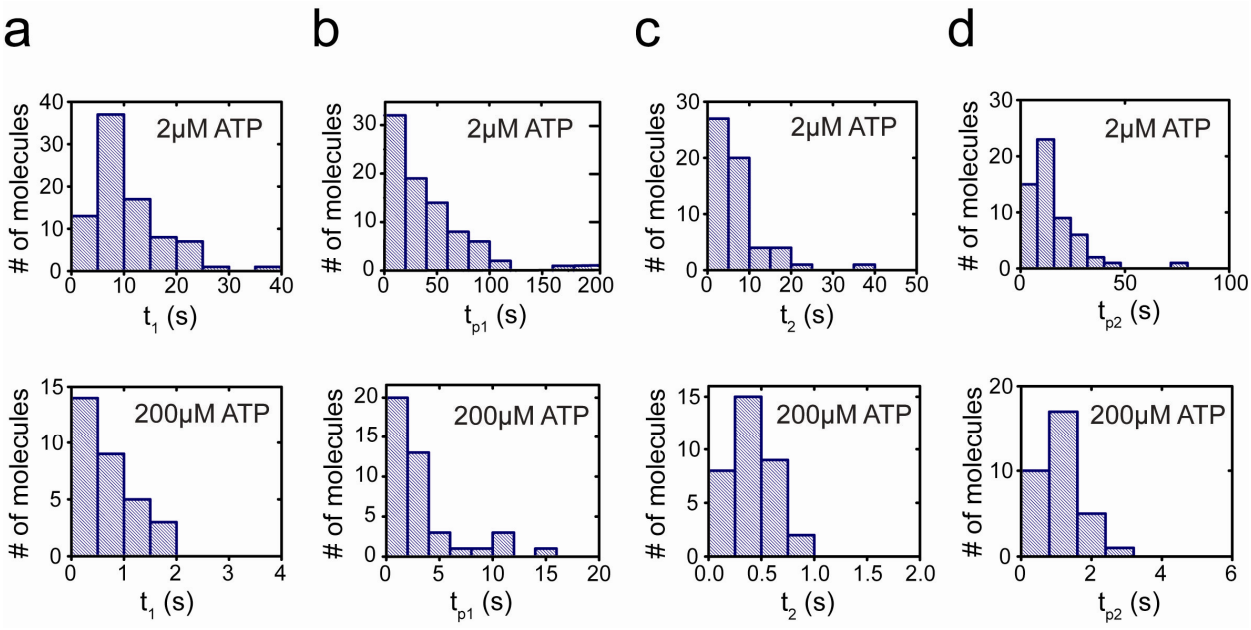

Supplementary Figure 8. Dwell time distributions of the first translocation phase t_1, the first pause t_{p1}, the second translocation phase t_2, and the second pause t_{p2} at various ATP concentrations. **a,** Dwell time distributions of t_1. **b,** Dwell time distributions of t_{p1}. **c,** Dwell time distributions of t_2. **c,** Dwell time distributions of t_{p2}. The mean values of t_1, t_{p1}, t_2, and t_{p2} at these and additional ATP concentrations are shown in Fig. 3e.

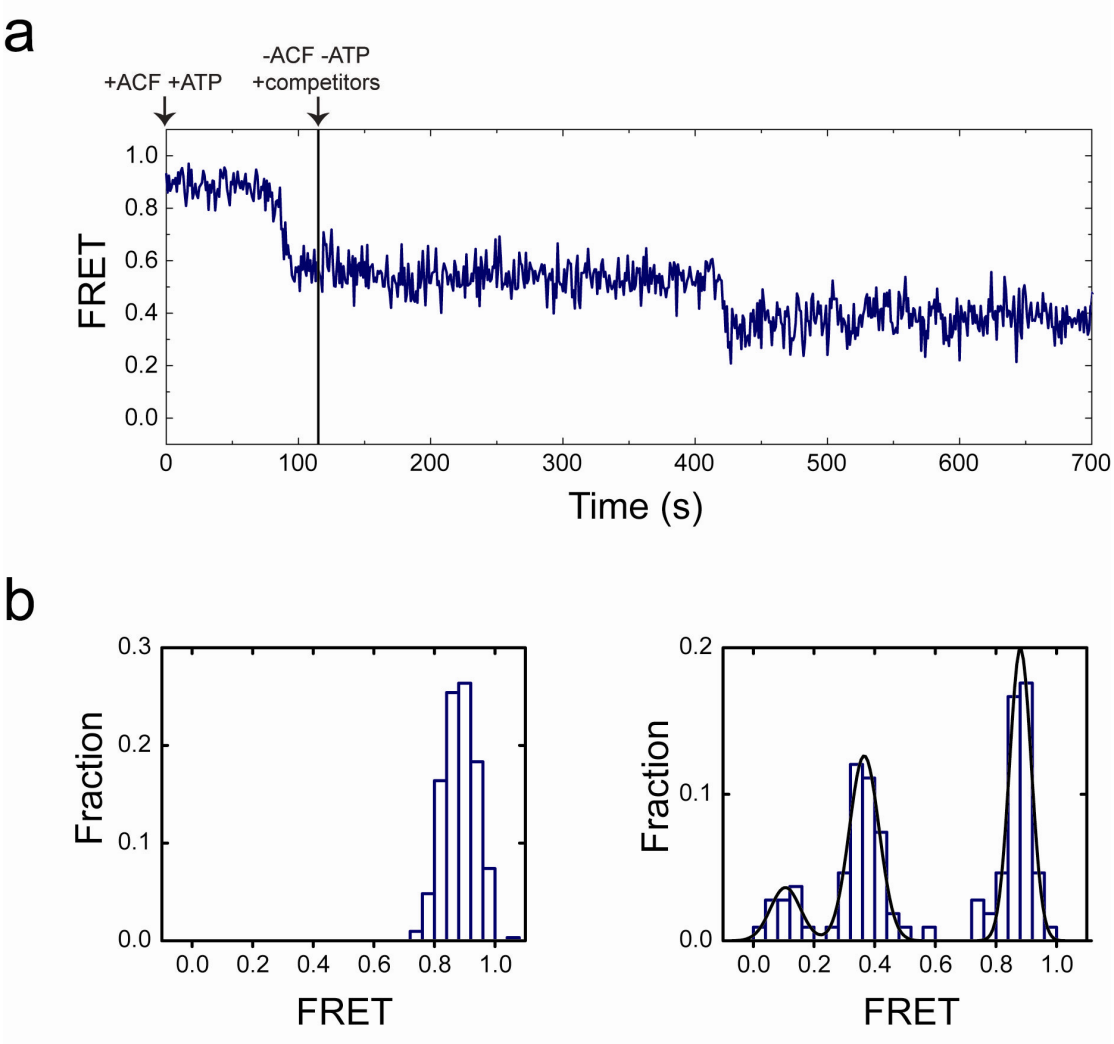

Supplementary Figure 9. Relaxation of the remodelling intermediates to more stable nucleosomal states upon removal of ACF. In this experiment, nucleosomes with initial exit linker length n = 3 bp were subject to remodelling by ACF. ACF (15 nM) and ATP (2-3 μM) were added at time zero to initiate remodelling. The enzyme and ATP were then chased out at time = 115 s by buffer exchange with a solution containing 2 mM ATPγS and 1 mg/ml plasmid DNA as competitors. The nucleosomes were allowed to relax in the absence of the ACF enzymes for 10 minutes. **a,** FRET time trace of a nucleosome showing ACF-induced nucleosome translocation as indicated by the decrease in FRET, a translocation pause at FRET = 0.53 corresponding to 7 bp of nucleosome translocation, and relaxation to a more stable nucleosomal state with a new FRET level (FRET = 0.37) after removal of ACF and ATP (black line). This final FRET level corresponds to 10 bp of translocation from the initial, pre-remodelling

nucleosomal state. **b,** FRET histograms of the nucleosomes before addition of ACF and ATP (left panel) and 10 minutes after removal of ACF and ATP (right panel). Nucleosomes with a FRET donor on the proximal H2A were selected for analysis, exhibiting FRET values centred at 0.88 before remodelling (left panel). After remodelling by ACF for 115 s and removal of the enzyme to allow nucleosome relaxation for 10 minutes, the FRET distribution exhibits three distinct peaks (right panel, blue bars). The histogram was fit to three Gaussian functions (black line) to determine the peak positions. The peak at the highest FRET value (FRET = 0.88) is identical to the initial FRET before remodelling, corresponding to unremodelled nucleosomes. The middle peak (FRET = 0.37) corresponds to a final exit linker length of 13 bp, and thus 10 bp of translocation from the initial nucleosomal state. The lowest peak (FRET ~ 0.1) is comparable to the FRET obtained from nucleosomes with exit linker length n = 23 bp, which corresponds to ~20 bp of translocation from the initial state, though this quantification is less accurate due to the low sensitivity of FRET to distance change at very low FRET values.

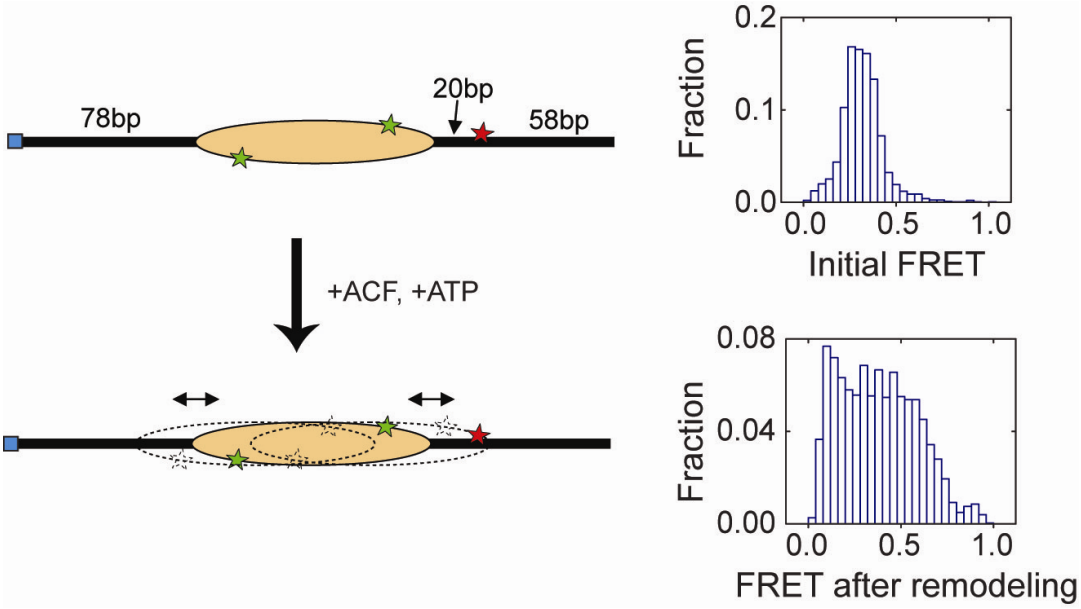

Supplementary Figure 10. FRET distribution of centre-positioned nucleosomes before and after remodelling by ACF. A centre-positioned nucleosome was flanked by 78 bp of linker DNA on both sides (left panel). The FRET distributions of nucleosomes prior to and after equilibration with 5 nM ACF and 2 mM ATP are shown in the upper and lower right panels, respectively.

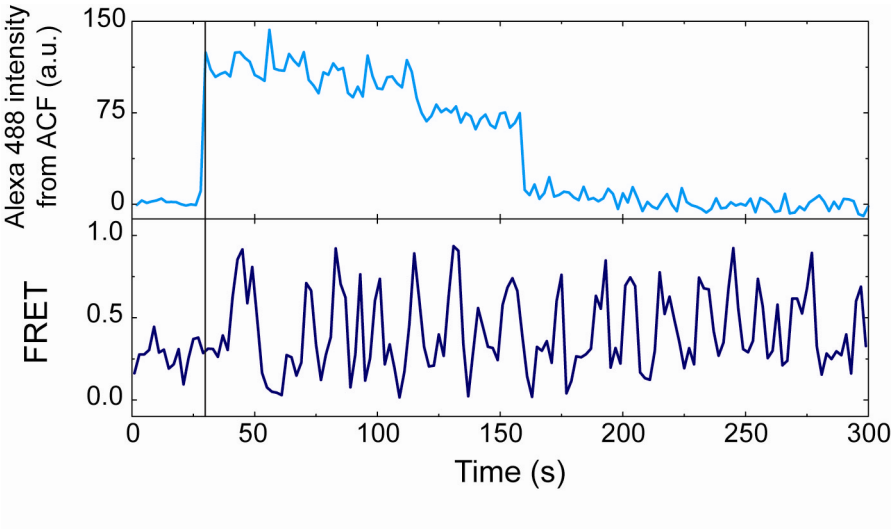

Supplementary Figure 11. Three-colour experiment showing back-and-forth nucleosome translocation within single ACF binding events. In this experiment, ACF was labelled with blue Alexa 488 dye and the centre-positioned nucleosomes flanked by 78 bp DNA linkers on both sides were labeled with a FRET donor Cy3 and acceptor Cy5 (See Fig. 4a). Signal from the Alexa 488 dye (upper panel) reports the binding of ACF to the nucleosome, while the FRET signal between Cy3 and Cy5 (lower panel) reports the position of the octamer on the DNA. The FRET trace shows multiple oscillations, indicating back-and-forth movement of the nucleosome, during a single ACF binding event that started at time = 29 sec (black line). The ACF signal shows a two-step decrease toward the background level consistent with the bleaching of two Alexa 488 dyes. The decrease in the Alexa 488 intensity is unlikely due to dissociation of ACF as the back-and-forth nucleosome movement continued even after the Alexa 488 signal was reduced to the background level.

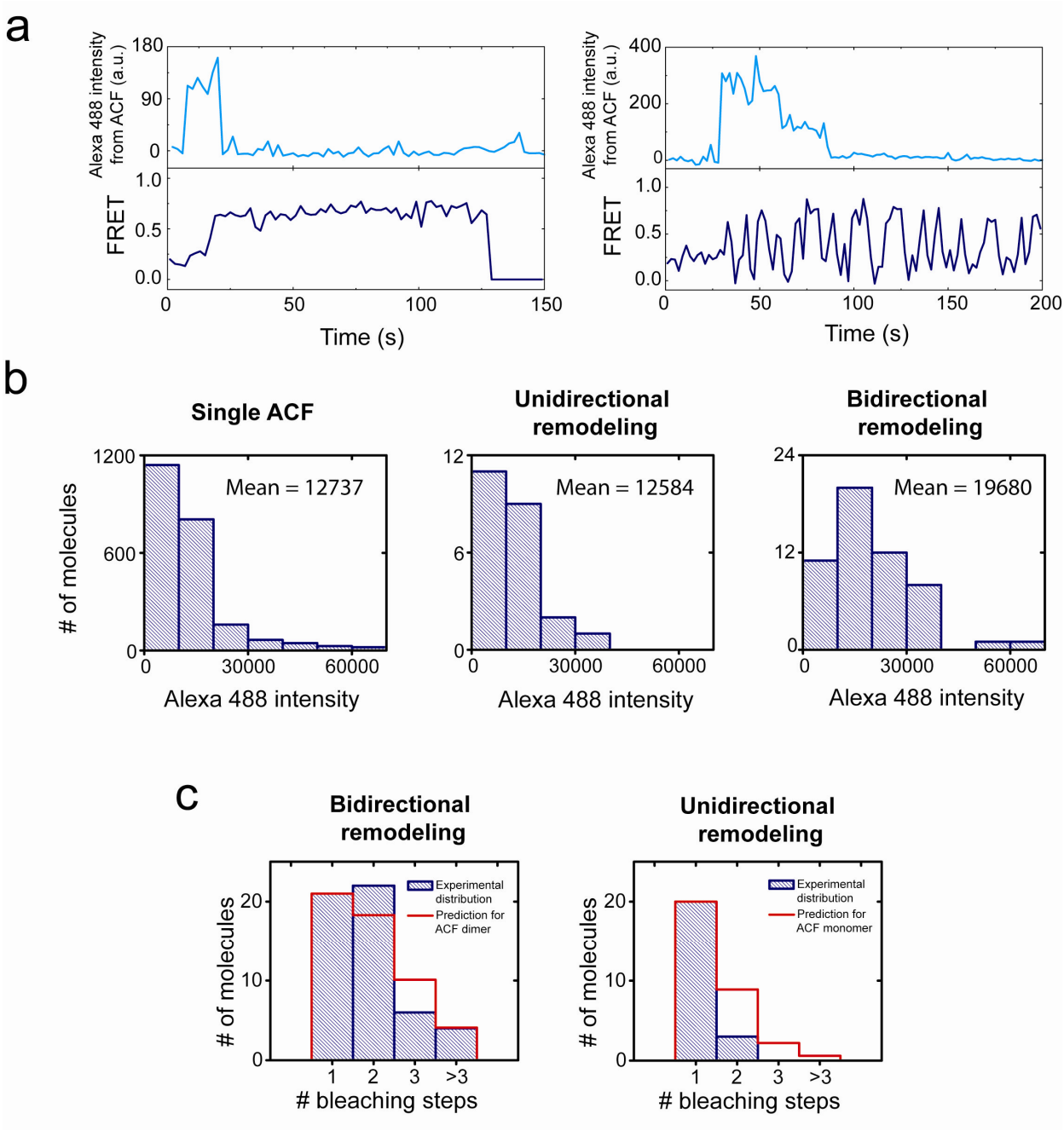

Supplementary Figure 12: Intensity and photobleaching step analyses of dye-labeled ACF associated with the unidirectional and bidirectional nucleosome remodelling events. In this experiment, ACF was labelled with Alexa 488 and the centre-positioned nucleosomes were labeled with FRET donor Cy3 and acceptor Cy5. **a**, Time traces of the Alexa 488 intensity and Cy3-to-Cy5 FRET associated with a unidirectional remodelling event (left) and a bidirectional remodelling event (right). The Alexa 488 signals from ACF are shown in the upper panels; the

FRET values from the nucleosomes are shown in the lower panels. **b**, The Alexa 488 intensity distributions for individual ACF enzymes bound to a surface (left panel), ACF complexes bound to nucleosomes exhibiting unidirectional movement (middle panel), and ACF complexes bound to nucleosomes exhibiting bidirectional movement (right panel). The observed intensity distribution of ACF bound to nucleosomes exhibiting unidirectional movement is quantitatively similar to that of individual ACF enzymes bound to a surface. The mean Alexa 488 intensities in the two cases are identical to each other within 1%. These results suggest that the unidirectional remodelling events were preferentially cause by ACF monomers. In contrast, the intensity of ACF bound to nucleosomes exhibiting bidirectional movement is substantially higher, with a mean Alexa 488 intensity that is 1.6 times that measured for single ACF enzymes. To quantitatively interpret the 1.6 fold higher Alexa 488 intensity, we estimated the number of Alexa 488 dyes per ACF. The non-specifically labelled ACF has a dye-to-enzyme ratio of 0.85. Considering the large number of potential labelling sites on ACF (41 cysteines), the number of dye molecules per ACF should follow a Poisson distribution with a mean of 0.85. This corresponds to 43% of enzymes unlabelled, 36% labelled with one dye, 16% with 2 dyes, 4% with 3 dyes, and 1% with more than 3 dyes. Among the binding events that exhibit detectable ACF signal (this excludes binding events of unlabelled ACF), the average number of associated Alexa 488 molecules should be 1.4 if ACF binds as a monomer, and 2.0 if ACF binds as a dimer. The ratio of 2/1.4 is similar to the 1.6 ratio observed for the mean intensity of ACF bound to nucleosomes exhibiting bidirectional movement versus that of single ACF bound to a surface, suggesting that bidirectional nucleosome movement is preferentially caused by ACF dimers. **c**, The statistical distributions of the Alexa 488 photobleaching steps associated with ACF bound to nucleosomes exhibiting bidirectional (left panel) and unidirectional (right panel) movement. The experimental data (blue shaded bars) are compared with the theoretical predictions of the distribution of photobleaching steps for an ACF dimer (red hollow bars, left panel) and monomer (red hollow bars, right panel) derived using the Poisson distribution described earlier. Again, binding events of unlabeled ACF are excluded from the analysis. (left panel) The number distribution of Alexa 488 photobleaching steps associated with nucleosomes exhibiting bidirectional movement is quantitatively similar to the distribution predicted for an ACF dimer. According to the Kolmogorov-Smirnov test, the experimental distribution is statistically different from those predicted for an ACF monomer and trimer with 84% and 99% confidence,

respectively, whereas the difference between the experimental distribution (blue bars) and the prediction for an ACF dimer (red bars) is statistically insignificant (<1%). These results again suggest that bidirectional nucleosome movements were caused by ACF dimers. (right panel) The observed number distribution of Alexa 488 "photobleaching" steps associated with nucleosomes exhibiting unidirectional movement appears fewer than that predicted for an ACF monomer. The former mostly shows a single-step decrease to zero. Interestingly, the duration of these "single-step-to-zero" events (8 s on average) is substantially shorter than the time it takes to photobleach an Alexa 488 molecule (39 s on average), while the duration of individual decreasing steps observed for ACF associated with bidirectional remodelling events is comparable to the photobleaching time. These results suggest that the observed disappearance of Alexa 488 signal in the case of unidirectional remodelling is due to ACF dissociation rather than photobleaching of the dye, and that ACF monomers bind to nucleosomes with substantially lower affinity than ACF dimers.